Hindawi
International Journal of Photoenergy
Volume 2021, Article ID 6623776, 8 pages
https://doi.org/10.1155/2021/6623776

Research Article

Fabrication of SiC@Cu/Cu Composites with the Addition of SiC@Cu Powder by Magnetron Sputtering

Zhang Yunlong,[1,2] **Li Wenbo**,[1,2] **Hu Ming**,[1] **Yi Hongyong**,[1] **Zhou Wei**,[2] **Ding Peiling**,[1] **and Tang Lili**[1]

[1]*College of Materials Science & Engineering, Jiamusi University, Jiamusi 154007, China*
[2]*Anyang Institute of Technology, Anyang 455000, China*

Correspondence should be addressed to Hu Ming; huming1962@126.com and Yi Hongyong; yidianskate@163.com

Received 26 October 2020; Revised 24 January 2021; Accepted 17 February 2021; Published 26 February 2021

Academic Editor: Jinlong Liu

In view of the surface engineering application of electrical contact materials, SiC ceramic particles were introduced into copper matrix composites by the hot-press sintering method for the sake of enhancing the service life of copper matrix electrical contact materials. Magnetron sputtering technology was exploited to form the continuous copper film on the β-SiC powders in order to improve interface wettability between SiC powder and copper matrix. The SiC@Cu powders were treated by magnetron sputtering technology. Then, dynamic deposit behavior was described according to SEM results. The phase constitution, fracture morphology, relative density, porosity, Vickers hardness, and coefficient of thermal expansion of SiC@Cu/Cu composites with different SiC@Cu addition were analyzed in detail. The results showed that SiC@Cu powders with higher fraction in the SiC@Cu/Cu composites would decrease relative density and increase porosity, so it resulted in improvement of Vickers hardness. The addition of SiC@Cu decreased CTE values of the SiC@Cu/Cu composite, especially at high-level fraction SiC@Cu powder.

1. Introduction

Electrical contact material was one of the most important materials of the current transmission and conversion process, which was the core component and key surface engineering material. Electrical contact material had wider applications including motor, switches, relays, and connectors. These basic components of electrical contact were extensively applied in the field of information engineering, household electrical appliances, automotive engineering, and so on. The main performance of the above-mentioned electrical contact device would directly affect the reliability, stability, accuracy, and service life. Recently, the tendency of high precision and miniaturization for the various types of electrical contact devices was developed to meet higher performance requirement. Electrical contact devices should possess predominant performance such as better electrical resistivity and contact resistance, low density, high hardness, chemical composition, anticorrosion, connectivity, and structure reliability [1, 2].

The material properties determined the breaking capacity and reliability of an electric contact switch. The electrical contact material was the traditional noble metal (for Ag, Au, and Pt) and their alloys. However, the shortcoming such as high cost and shorter service life limited the wider application for these kinds of electrical contact materials. Compared with Ag system alloys, the copper series alloys had more superior high-temperature performance. In view of the surface engineering application of copper matrix electrical contact materials, SiC ceramic particles were introduced into the copper matrix in order to improve the hardness and friction resistance, whereas it was difficult to resolve the weak wettability between the SiC reinforcement and copper matrix, which limited the wider application scope of copper composites [3, 4]. Recently, the surface modification technologies were developed to improve the interface binding properties,

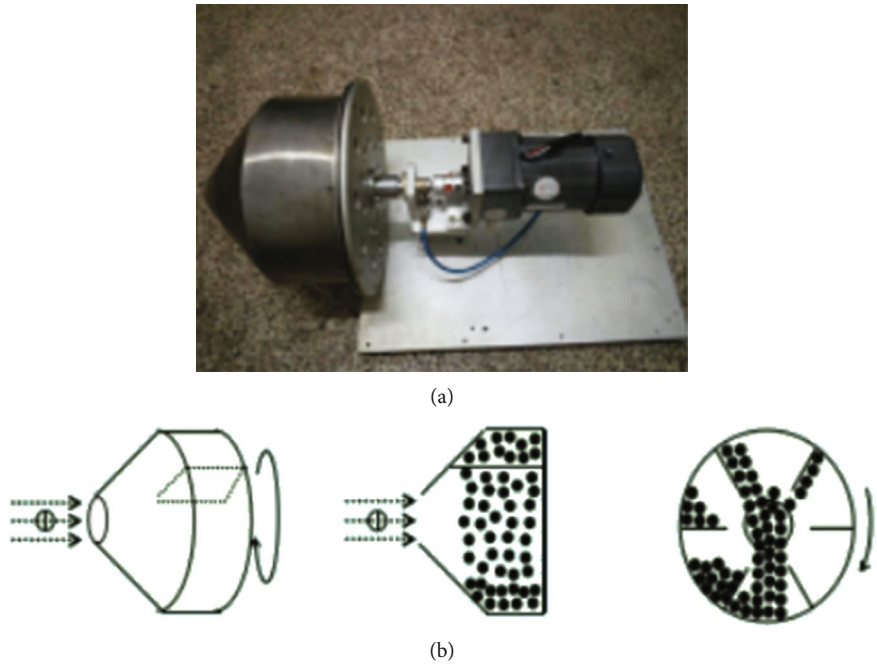

Figure 1: The physical picture self-designed carrier (a) and schematic diagram of the magnetron sputtering process (b).

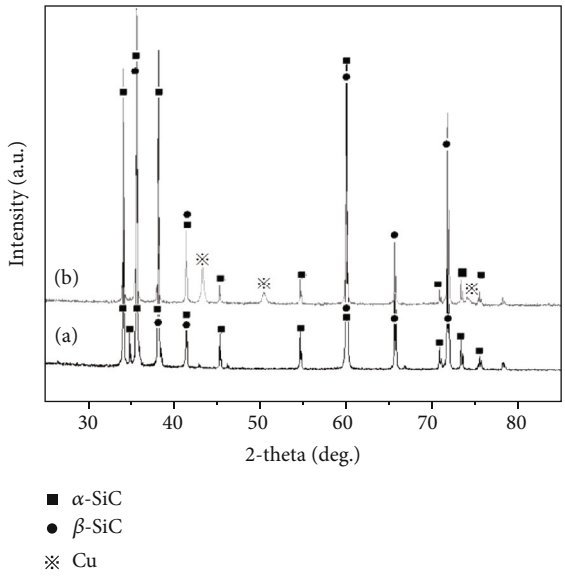

Figure 2: XRD curve of SiC particles and SiC@Cu powder: (a) XRD curve before magnetron sputtering and (b) XRD curve after magnetron sputtering.

for example, electroless plating, sol-gel and plasma modification, and magnetron sputtering [5–9]. At present, the magnetron sputtering deposition method was widely investigated as an important surface modification method. The magnetron sputtering technology was investigated to form the thin coating and/or films on the different substrate materials [10]. However, the reports about magnetron sputtering films on the surface of SiC ceramic particles were scarce. For the sake of enhancing the service life of copper matrix electrical contact materials, we attempt to utilize magnetron sputtering technology to obtain the copper film on the surface of the SiC particle (abbreviation "SiC@Cu"). High-volume fraction SiC@Cu powder in the Cu matrix composites had attracted much attention in thermal management application, which exhibited high thermal conductivity, low thermal expansion, excellent mechanical properties, and better wear resistance [11, 12]. Hot pressing sintering route was a main adopted technique in order to obtain the more dense SiC@Cu/Cu hybrid materials.

In the present investigation, we put focus on the preparation of SiC@Cu powders with copper coating by means of the magnetron sputtering method. The preliminary result was reported by the previous article [13]. Other target was aimed at fabricating SiC@Cu/Cu composites with different SiC@Cu volume fractions. The influence of SiC@Cu fraction on the thermal physical properties of the SiC@Cu/Cu composites was analyzed. The SiC@Cu/Cu composites were fabricated at 750°C for 1 h by the hot-press sintering method. The phase constitution, fracture and surface morphology, relative density, porosity, Vickers hardness, and coefficient of thermal expansion of the SiC@Cu/Cu composites with different SiC@Cu volume fractions were observed and analyzed in detail.

2. Material Fabrication and Characterization

The magnetron sputtering equipment was used to generate copper films on the surface of the SiC particle. The target material used for sputtering was Cu target (purity 99.999%) with a diameter of 100mm and a thickness of 5mm. The target material was placed on the target frame connected with the cooling circulating water device. The self-designed circular carrier was used to load SiC powder and was put on the holder. The physical picture and schematic diagram of the

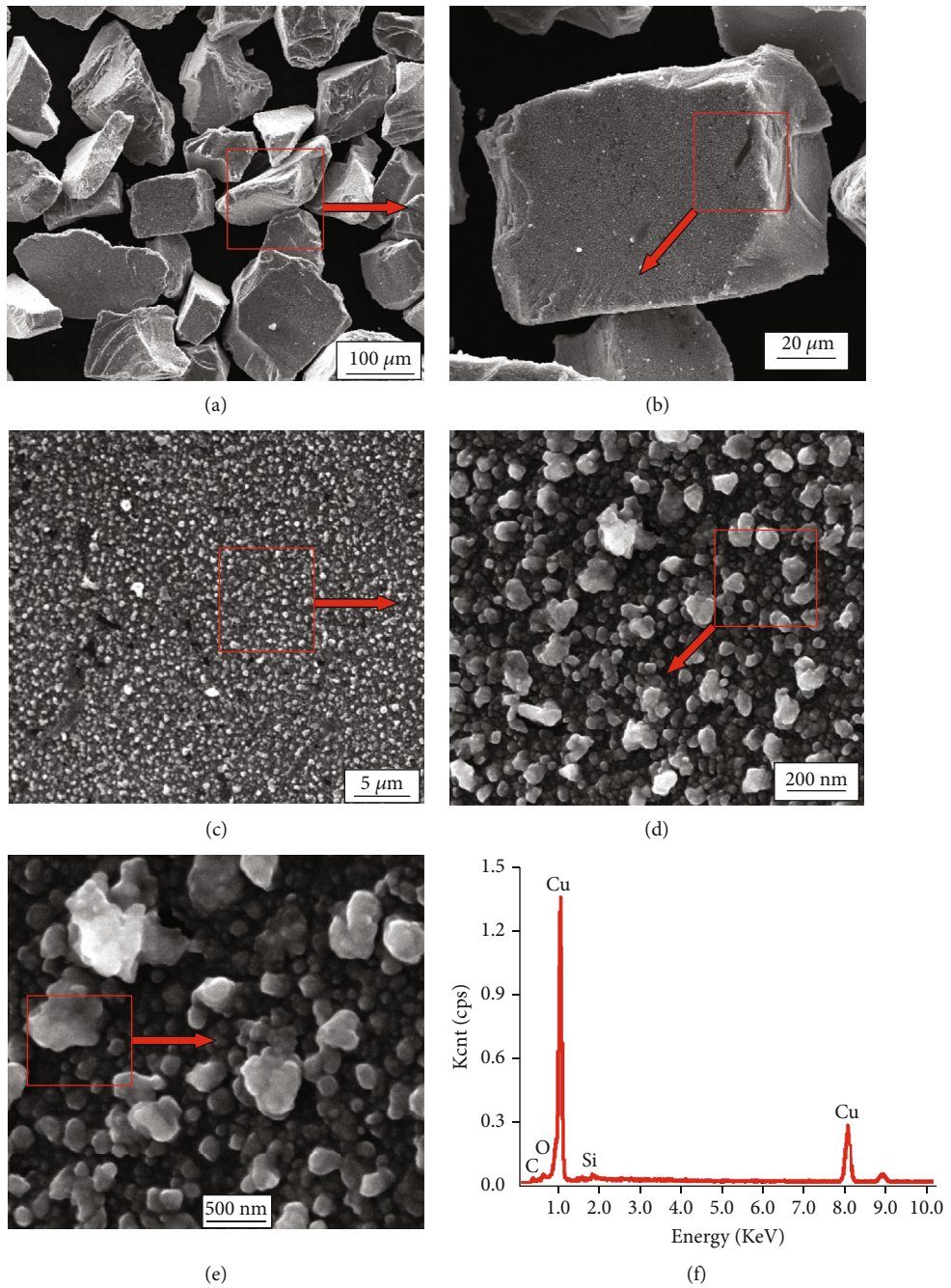

FIGURE 3: Morphology of the copper film on β-SiCp after magnetron sputtering was formed. β-SiCp with the copper film at low magnification (a) and high magnification (b–e) and energy pattern (f).

self-designed carrier are shown in Figure 1. By adjusting the swing frequency of the specimen holder and the vibration power of the ultrasonic wave, SiC powder can roll horizontally and vibrate vertically to ensure that the surface of each particle can be coated with a copper film evenly. β-SiC powders ($D_{50} = 78\mu$m) were set into the loading powder container, and the target distance was about 150mm. The vacuum pressure was suction filtration to 10^{-3}Pa. The argon gas was introduced into reaction equipment with flow 20 sccm, and puttering pressure was about 1.0Pa. Sputtering power was set as 370W and sputtering time set as 90 min. The temperature was controlled in the scope of 25~150°C. The sample holder with low-frequency swing and ultrasonic wave with high-frequency oscillation were applied to ensure uniform distribution of the copper film on the surface of SiC particles. SiC powders with the Cu film were defined as SiC@Cu powders. The nitric acid impregnation method was applied to calculate the gained copper weight on SiC@Cu powders. After calculation, gained copper weight on the sputtered powders was about 2.2%. SiC@Cu powders and copper powders were mixed by ball milling equipment. The volume ratio of SiC@Cu powders to total mixed powders

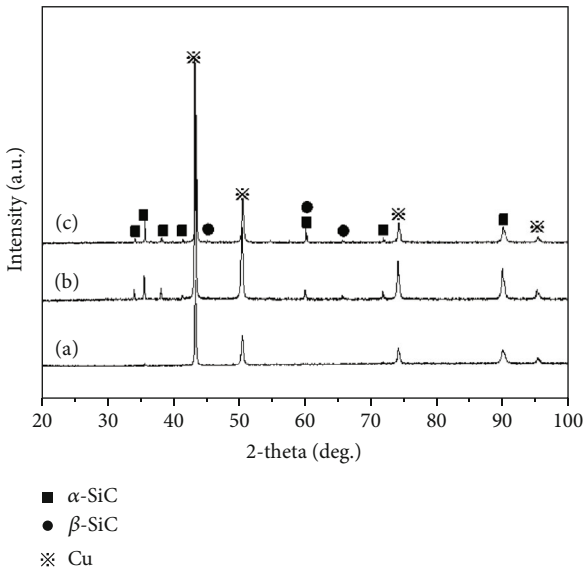

Figure 4: XRD curve of SiC@Cu/Cu composites. (a), (b), and (c) presented the SiC@Cu volume fraction with 10%, 30%, and 50%.

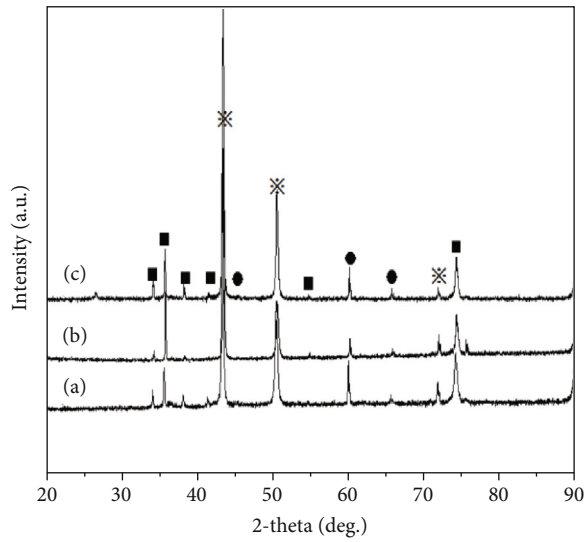

Figure 5: XRD curve of SiC_p/Cu composites with different SiC_p fractions without magnetron sputtering. (a), (b), and (c) presented the SiC_p volume fraction with 10%, 30%, and 50%.

was adjusted as 0%, 10%, 20%, 30%, 40%, and 50%, and the above specimen was named as S0, S10, S20, S30, S40, and S50 ("S" was the abbreviation of "specimen"). The ball milling speed was 300 r/m, and the time was set as 8 h. Prior to the sintering process, the mixture powders was cold-pressed into a cylindrical compact in a metal die of 40 mm in diameter with pressure of 200 MPa. SiC@Cu/Cu composites were sintered at 750°C for 60 min in a multifunctional hot-pressing sintering furnace with argon gas protection, and the heating rate was about 20°C/min. The sintered SiC@Cu/Cu composites were cut into 3 mm × 3 mm × 4 mm for morphology observation. The phase composition of SiC powders and SiC@Cu/Cu composites was identified by X-ray diffraction (D8 Advance, Germany). The scanning speed was 4°/min, and the step length was 0.02°. The morphology of SiC powders with copper films was observed by SEM (Hitachi S4700). Relative densities were calculated according to Archimedes' principle. To determine the microhardness of SiC@Cu/Cu composites, the Vickers indentor was applied with a load of 196 N for 15 s on the polished surface by using a hardness testing machine. The thermal expansion tester (Netzsch-DIL402C) was selected to survey the CTE of SiC@Cu/Cu composites, and the measuring temperature was varied in 25°C~00°C; then, the average value of CTE was obtained. As a comparative test analysis, SiC particles without magnetron sputtering were directly introduced into the copper matrix with volume fractions of 10%, 20%, 30%, 40%, and 50%, respectively, which were named as RS10, RS20, RS30, RS40, and RS50 ("RS" was the abbreviation of "received specimen"). The sintering process and result characterization process were the same as above.

3. Result and Discussion

The XRD curve of SiC powders before magnetron sputtering deposition is shown in Figure 2(a). As seen from original SiC powder, the β-SiC phase can be detected. At the same time, the α-SiC phase can be detected. The possible reason was that the phase of received powder was made up of the β-SiC phase and α-SiC phase. After magnetron sputtering deposition, SiC@Cu powders can be detected in Figure 2(b). The high sputtering yield of copper can be obtained, and the high deposition rate was gained by adjusting sputtering parameters such as temperature, time, and sputtering power. It is worth noting that obvious copper aggregate structure was detected as the sputtering power and/or matrix temperature was too high. So it was beneficial for acquiring uniform and suitable film thickness for copper on the SiC surface by adjusting appropriate magnetron sputtering parameters.

The surface morphology of SiC@Cu powder is illustrated in Figure 3. It needs to be stressed that the growth rate of the copper film on the SiC_p surface in the motion process was similar to that on the flat substrate. The copper film was composed of bigger grains and smaller grains. It was interesting that vast bigger grains were composed of dozens of smaller grains with tens of nanometers, whose shape was the same as an isolated island. The size of "Volmer-Weber" grains was about 200~500 nm. The nucleation rate of copper formation and growth rate of nuclear island enhanced as the sputtering time increased. The higher temperature of SiC powders improved diffusion capacity of copper atoms, and it was beneficial for the formation of the thicker copper film. The process and growth mechanism of magnetron-sputtered copper films had been discussed in reference [14].

The phase constitutions of SiC@Cu/Cu composites with different SiC@Cu fractions after magnetron sputtering are illustrated in Figure 4(a), (b) and (c) in Figure 4 present the volume fraction of SiC@Cu with 10%, 30%, and 50%. The main phase for SiC@Cu/Cu composites was the α-SiC, β-SiC, and Cu phase. The initial pure copper was tested as shown in Figure 4(a). It was seen from Figure 4(b) and (c) that there was no other component except Cu and SiC in the SiC@Cu/Cu composites.

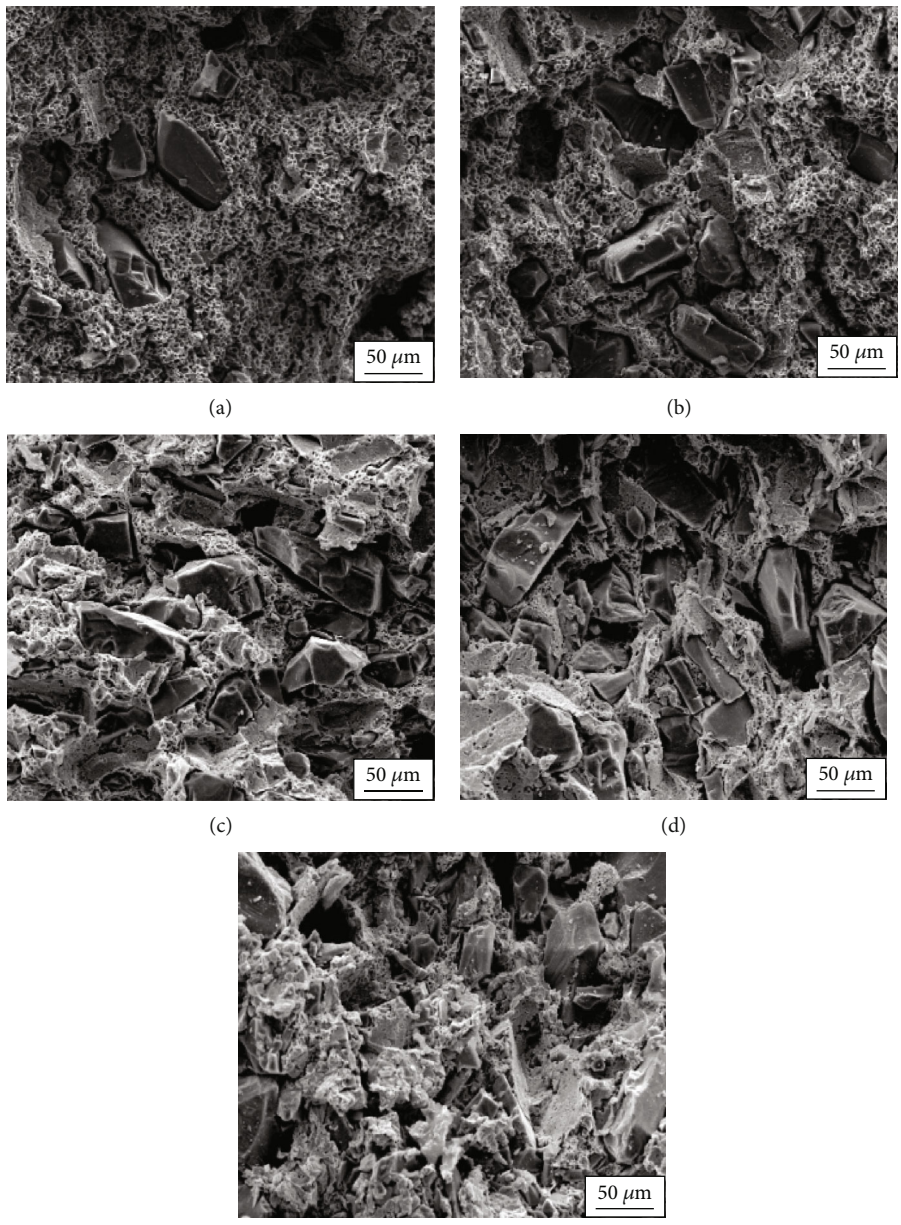

Figure 6: Fracture surface of SiC@Cu/Cu composites with different SiC@Cu fractions: (a–e) SiC@Cu fraction with 10%, 20%, 30%, 40%, and 50%.

Table 1: Vickers hardness and relative density of the SiC@Cu/Cu composite.

Specimen	S0	S10	S20	S30	S40	S50
Relative density	99.6%	98.8%	98.1%	97.7%	97.2%	96.5%
Vickers hardness (kgf/mm^2)	35 ± 2.4	62 ± 2.5	74 ± 2.6	95 ± 2.4	108 ± 3.2	132 ± 2.7

Table 2: Vickers hardness and relative density of the SiC_p/Cu composite.

Specimen	RS10	RS20	RS30	RS40	RS50
Relative density	98.4%	97.8%	97.2%	96.9%	96.3%
Vickers hardness (kgf/mm^2)	56 ± 3.2	70 ± 2.6	92 ± 2.8	101 ± 3.1	125 ± 3.5

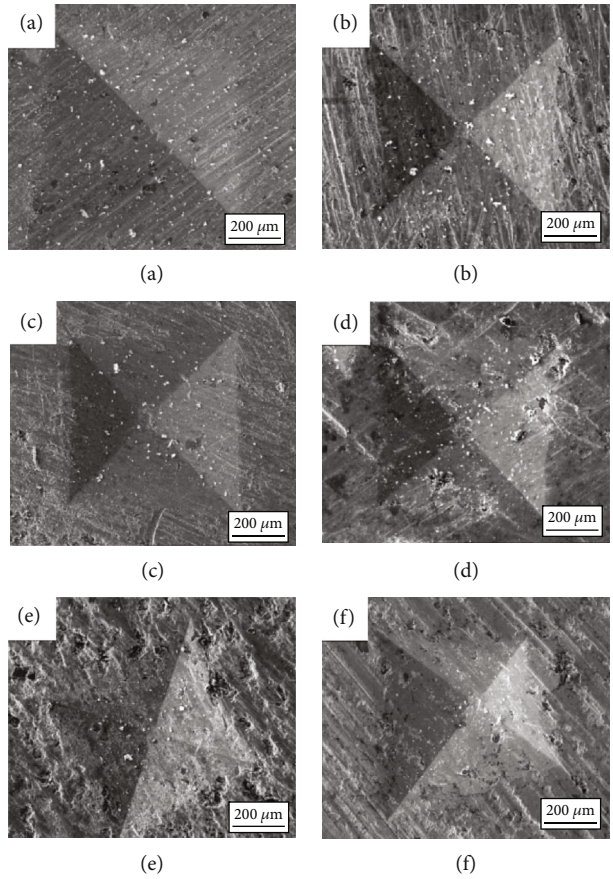

Figure 7: Vickers indentation of the SiC@Cu composites with different SiC@Cu fractions.

Figure 5 displays the XRD curve of SiC_p/Cu composites with different SiC_p fractions. Figure 5(a)–(c) present the SiC_p fraction with 10%, 30%, and 50%. SiC peaks became clear with the increasing SiC_p fraction. As a contrast specimen, XRD results of SiC_p/Cu composites with the same amount of SiC added showed the same phase composition and similar diffraction peaks. Under the same addition amount of SiC, the diffraction peak strength of SiC in the SiC hybrid copper-matrix composites without magnetron sputtering was slightly enhanced. The possible reason was that the copper film effect of the SiC surface was more uniform after magnetron sputtering treatment, so the bonding role between the SiC@Cu powder and copper matrix became stronger in the sintering process. The content of SiC on the exposed surface was relatively low after grinding and polishing before detection. Therefore, the diffraction peak intensity was lower.

The fracture surface of SiC@Cu/Cu composites with different SiC@Cu fractions is shown in Figure 6. As the SiC@Cu fraction was lower than 20%, the ductile rupture at the copper matrix was mainly the fracture mechanism. As the SiC@Cu fraction was higher than 30%, the ductile rupture at the copper matrix and debonding of the SiC/Cu interface were mainly the fracture behaviors. As the SiC@Cu fraction was higher than 30%, more SiC@Cu particles can be seen on the fracture surface. Pulling out of SiC particles and big dimples was clearly found on the fracture surface. Then, SiC@Cu/Cu composites exhibited a brittle fracture mechanism. Some SiC particles gathered with pores were observed. It was revealed that interfacial bond was weak in the near pore region. It can be concluded that weaker bonding strength of the SiC/Cu interface was the primary factor, which was responsible for relatively low flexural strength. Debonding of the SiC/Cu interface was lessened and particle pulling out from copper matrix was not obvious on the fracture surface. Severe ductile deformation in the copper matrix was the main fracture mechanism of SiC@Cu/Cu composites with a lower SiC@Cu fraction.

Test results of relative density and Vickers hardness of SiC@Cu/Cu composites are listed in Table 1. The relative density decreased with the volume fraction of SiC@Cu increasing. For all SiC@Cu composites, relative density was higher than 96%. Even if the SiC@Cu fraction reached 50%, the relative density was about 96.5%. In the SiC@Cu composite with a lower SiC@Cu volume fraction, less interface between Cu and SiC@Cu meant less copper atom diffusion barrier and copper atoms diffused conveniently and filled the interstices between SiC particles; then, it resulted in higher densification. So it can draw to a conclusion that the hot-press sintering method was effective to fabricate compact SiC@Cu/Cu composites. The Vickers hardness of SiC@Cu/Cu composites increased as the volume fraction of SiC@Cu powders increased. The Vickers hardness of sintered pure copper was about 35 kgf/mm^2. When the volume fraction of SiC@Cu reached 50%, the Vickers hardness of

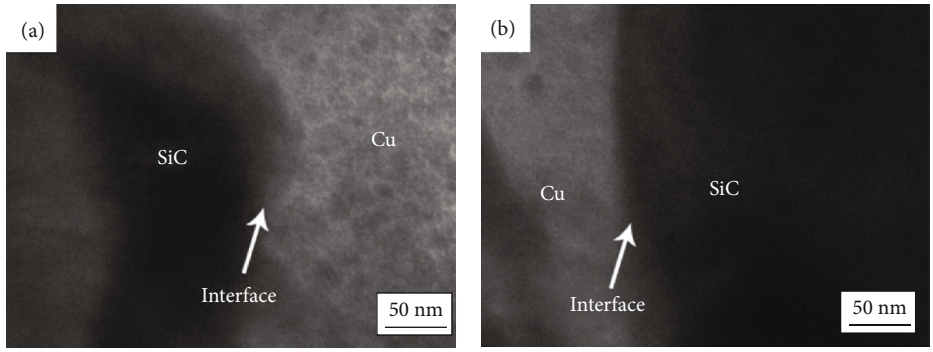

(a) (b)

Figure 8: TEM photo of SiC@Cu/Cu composites: (a) 10% SiC@Cu and (b) 30% SiC@Cu.

SiC@Cu/Cu composites was nearly 132 kgf/mm^2. Therefore, introduction of SiC@Cu improved the Vickers hardness of the SiC@Cu/Cu composite, especially at the high fraction of SiC@Cu powder.

Test results of relative density and Vickers hardness of SiC_p/Cu composites with different fractions of SiC_p are shown in Table 2. The relative density decreased with the volume fraction of SiC_p increasing. The relative density varied in the range of 96.3% and 98.4%. The microhardness corresponding to RS10, RS20, RS30, RS40, and RS50 was 56 kgf/mm^2, 70 kgf/mm^2, 92 kgf/mm^2, 101 kgf/mm^2, and 125 kgf/mm^2, respectively. At the same volume fraction, the relative density of the SiC@Cu/Cu composite was higher than that of the SiC_p/Cu composite. The Vickers hardness of the SiC_p/Cu composite decreased with the increase in the volume fraction of SiC_p powder.

Vickers indentation of SiC@Cu/Cu composites is shown in Figure 7. With the increase in the SiC@Cu fraction, the depth of Vickers indentation for SiC@Cu/Cu composites became shallower. It can be concluded that the second-phase introduction of SiC@Cu powders improved the Vickers hardness of SiC@Cu/Cu composites. It was thought that higher amount of ceramic particles in the copper matrix resulted in more dislocations and the dislocations lead to the increase in hardness of SiC@Cu/Cu composites. The relative density and Vickers hardness of the SiC_p/Cu composite were lower than those of the SiC@Cu/Cu composites, which was related to the bonding degree of the magnetron-sputtered copper film and SiC particles.

TEM photo of SiC@Cu/Cu composites with different SiC@Cu fractions can be seen in Figure 8. Figures 8(a) and 8(b) present the volume fraction of SiC@Cu powder as 10% and 30%. The interdiffuse interface layers were stinct, which was diffused into the interior of the coating. The interdiffuse phenomenon was discovered in the other SiC@Cu/Cu composites. This kind of structure occurred in all SiC@Cu/Cu specimens. As the SiC@Cu fraction was low, the distribution of the structure was obvious. While the SiC@Cu fraction was higher than 40%, the discontinuous interface structure could be detected. It can be concluded that magnetron sputtering technology was an effective way to improve interface interdiffuse behaviors of SiC@Cu/Cu composites.

Figure 9 shows the survey on the relation curve between the SiC@Cu fraction and coefficient of thermal expansion

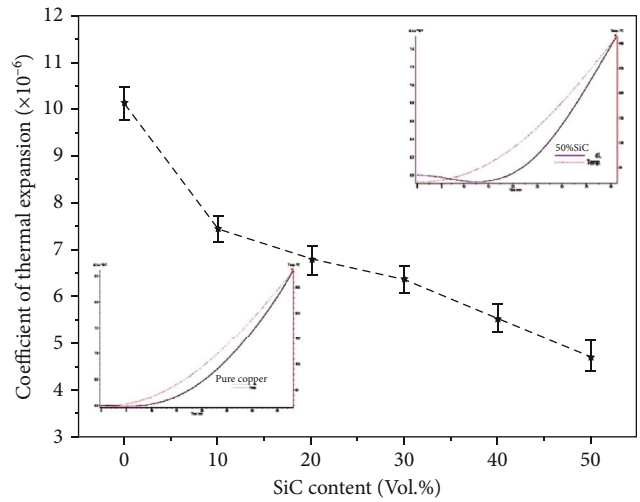

Figure 9: Relation curve between the SiC@Cu fraction and CET of SiC@Cu/Cu composites.

(abbreviation "CET") of the SiC@Cu/Cu composites. It was expected that CTE of SiC@Cu/Cu composites lowered with the introduction of SiC@Cu powders. Figure 9 displays the mean CTE of all specimens in the range of 50°C~300°C. Within the entire investigated temperature range, CTE values decreased apparently with the increasing SiC@Cu fraction. The reduction of CTE was reckoned as the results of mixture rule and the intense restriction effect of SiC@Cu reinforcement on the copper matrix. The relative experiment proved that CTE values of SiC@Cu/Cu composites were lower than those of SiC_p/Cu specimens under the condition of the same doping amount of SiC. CTE values reflected the level of stress mismatched by introducing SiC@Cu reinforcement in the copper matrix.

4. Conclusion

In this thesis, magnetron sputtering technology was applied to obtain a continuous copper film on the SiC grains successfully. The dynamic formation mechanism of the copper film was a mixture model of main island structure growth and secondary layered structure growth as SiC grains moved

during the magnetron sputtering process. The hot-press sintering method was utilized to fabricate SiC@Cu/Cu composites at 750°C for 60 min. The relative density of SiC@Cu/Cu composites decreased as the SiC@Cu fraction increased. For all SiC@Cu/Cu composites, the relative density was higher than 96%. The Vickers hardness of SiC@Cu/Cu composites increased with the volume fraction of SiC@Cu powders increasing. According to TEM result, the interdiffuse phenomenon was discovered in the SiC@Cu/Cu composites. The introduction of SiC@Cu powder improved the Vickers hardness of the SiC@Cu/Cu composite, especially at the high SiC@Cu fraction level. CTE values decreased with the increasing volume fraction of SiC@Cu powders within the range of investigated temperature.

Data Availability

The data used to support the findings of this study are included within the article.

Disclosure

Part of the preliminary research work had been published in the journal "*Advances in Computer Science Research*, volume 71" (4th International Conference on Machinery Materials and Information Technology Applications in 2016).

Conflicts of Interest

The authors declare that they have no conflicts of interest.

Acknowledgments

The authors and collaborators were grateful for the support by the National Science Foundation of China (No. 51671096), Materials Science and Engineering Team Project of Jiamusi University (JDXKTD-2019001), and Scientific Research Project of the Education Department of Heilongjiang Province (2016-KYYWF-0556, 2019-KYYWF-1373). Meanwhile, the thesis was supported by Key Scientific Research Projects of Higher Education Institutions of Henan Province (Project number 18A430006) and Science and Technology Research Projects from Anyang City (Project "thermal conductivity behavior research of copper matrix hybrid materials with wear-resisting/low expansion for aviation electric contact field"). Part of the data in this paper was provided by "Key Laboratory of Aerocraft Simulation Design and Airborne Equipment of Anyang City".

References

[1] J. Zheng, S. Li, F. Dou, and T. Li, "Preparation and microstructure characterization of a nano-sized Ti^{4+}-doped $AgSnO_2$ electrical contact material," *Rare Metals*, vol. 28, no. 1, pp. 19–23, 2009.

[2] T. Varo and A. Canakci, "Effect of the CNT content on microstructure, physical and mechanical properties of Cu-based electrical contact materials produced by flake powder metallurgy," *Arabian Journal for Science and Engineering*, vol. 40, no. 9, pp. 2711–2720, 2015.

[3] R. Zhang, L. Gao, and J. K. Guo, "Preparation and characterization of coated nanoscale Cu/SiC_p composite particles," *Ceramics International*, vol. 30, no. 3, pp. 401–404, 2004.

[4] V. Martínez, S. Ordoñez, F. Castro, L. Olivares, and J. Marín, "Wetting of silicon carbide by copper alloys," *Journal of Materials Science*, vol. 38, no. 19, article 5252263, pp. 4047–4054, 2003.

[5] T. Schubert, A. Brendel, K. Schmid et al., "Interfacial design of Cu/SiC composites prepared by powder metallurgy for heat sink applications," *Composites Part A: Applied Science and Manufacturing*, vol. 38, no. 12, pp. 2398–2403, 2007.

[6] H. Bi, K. C. Kou, A. E. Rider, K. Ostrikov, H. W. Wu, and Z. C. Wang, "Low-phosporous nickel-coated carbon microcoils: Controlling microstructure through an electroless plating process," *Applied Surface Science*, vol. 255, no. 15, pp. 853–858, 2009.

[7] E. Neubauer, G. Kladler, C. Eisenmenger-Sittner et al., "Interface design in copper-diamond composite by using PVD and CVD coated diamonds," *Advanced Materials Research*, vol. 59, pp. 214–219, 2008.

[8] B. Wang, Z. Ji, F. T. Zimone, G. M. Janowski, and J. M. Rigsbee, "A technique for sputter coating of ceramic reinforcement particles," *Surface and Coatings Technology*, vol. 91, no. 1-2, pp. 64–68, 1997.

[9] H. Kersten, P. Schmetz, and G. M. W. Kroesen, "Surface modification of powder particles by plasma deposition of thin metallic films," *Surface and Coating Technology*, vol. 108, pp. 507–512, 1998.

[10] C. M. Fernandes, V. M. Ferreira, A. M. R. Senos, and M. T. Vieira, "Stainless steel coatings sputter-deposited on tungsten carbide powder particles," *Surface and Coating Technology*, vol. 176, no. 1, pp. 103–108, 2003.

[11] K. M. Shu and G. C. Tu, "The microstructure and the thermal expansion characteristics of Cu/SiC_p composites," *Materials Science and Engineering A*, vol. 349, no. 1-2, pp. 236–247, 2003.

[12] P. Yih and L. Chung, "Silicon carbide whisker copper-matrix composites fabricated by hot pressing copper coated whiskers," *Journal of materials science*, vol. 31, no. 2, pp. 399–406, 1996.

[13] D. Peiling, Z. Yunlong, and M. Hu, "Effect of SiC p (Cu) addition on the property of the SiC_p (Cu) /Cu composites," *Advances in Computer Science Research*, vol. 71, pp. 748–751, 2016.

[14] M. Hu, Z. Yunlong, S. Lin et al., "Dynamic Ddeposition of Nnanocopper Ffilm on the β-SiCp Ssurface by Mmagnetron Ssputtering," *Journal of Nanomaterials*, vol. 2015, Article ID 810986, 6 pages, 2015.